Lithuanian Journal of Physics, Vol. **58**, No. 4, pp. 295–306 (2018)

DECAY- AND EVOLUTION-ASSOCIATED SPECTRA OF TIME-RESOLVED FLUORESCENCE OF LHCII AGGREGATES

A. Gelzinis [a, b], Y. Braver [a, b], J. Chmeliov [a, b], and L. Valkunas [a, b]

[a] *Institute of Chemical Physics, Faculty of Physics, Vilnius University, Saulėtekio 9, 10222 Vilnius, Lithuania*

[b] *Department of Molecular Compound Physics, Center for Physical Sciences and Technology, Saulėtekio 3, 10257 Vilnius, Lithuania*

Email: leonas.valkunas@ff.vu.lt

Received 22 July 2018; accepted 15 October 2018

Non-photochemical quenching (NPQ) is responsible for the protection of the photosynthetic apparatus of plants from photodamage at high-light conditions. It is commonly agreed that NPQ takes place in the major light-harvesting complexes (LHCII), however, its exact mechanisms are still under debate. Valuable information about its molecular nature can be provided by measuring time-resolved fluorescence (TRF) spectra of LHCII complexes and their aggregates. Previously [Chmeliov et al., Nat. Plants 2, 16045 (2016)], we analysed the corresponding TRF spectra using the multivariate curve resolution method and proposed a three-state model to describe the spectroscopic data. Usually, such data is described in terms of global analysis resulting in decay or evolution-associated spectra. In this work, we apply such analysis to the TRF data of LHCII aggregates and show that, although mathematically feasible, it cannot be directly related to the physical kinetic model. Nevertheless, a careful examination supplemented with additional spectroscopic information still results in the same three-state model proposed before.

Keywords: time-resolved fluorescence, decay associated spectra, ligh-harvesting complex

PACS: 78.47.D-, 78.47.jd, 82.20.Wt

1. Introduction

Throughout the ages plants, algae and some bacteria have adapted their photosynthetic machinery to function efficiently in a wide range of environmental situations [1]. Though being different in nature, the photosynthetic apparatus of all these organisms exhibit similar design principles: its central element – the reaction centre – is surrounded by large light-harvesting antenna. The antenna pigment–protein complexes absorb solar radiation and funnel the generated electronic excitations towards the reaction centre, where they are used for charge separation, initiating subsequent steps of photosynthesis. The mutual arrangement of the pigment–protein complexes within the photosynthetic membrane, their internal composition and spectral properties are the key reason why photosynthetic organisms can strive both at low-light and at high-light conditions. The ability to survive in dark environments comes at a cost, however. Under strong sunlight the light-harvesting antennae can collect significantly more photons than the reaction centre can process. Such an over-excitation can in turn lead to the formation of highly reactive molecular compounds potentially capable of damaging the whole photosynthetic apparatus.

To prevent possible photodamage, plants utilize several regulatory mechanisms. The most efficient of them, acting on a molecular level, is denoted as non-photochemical quenching (NPQ) [2]. Its energy-dependent component (qE) manifests reversibly within seconds to minutes and safely dissipates the excess excitation energy as heat. According to the recent research, NPQ takes place in the major light-harvesting complexes (LHCII) of the photosystem II of higher plants [3], though

minor antenna complexes should also be considered [4].

We have recently investigated the temperature dependence of the time-resolved fluorescence (TRF) of LHCII trimers and their aggregates [5]. In LHCII aggregates, the mean excitation lifetime is significantly reduced when compared to that of the trimers, and, additionally, at low temperatures a spectral feature at around 700 nm appears. Similar effects are observed in the intact thylakoid membranes [6, 7], which makes LHCII aggregates a good model system to mimic NPQ *in vivo*. In order to describe both our experimental observations as well as single-molecule spectroscopy data [8, 9], one must assume that at least three distinct macroscopic states are present within the LHCII aggregate: the dominating one, which exhibits a strong fluorescence peak at around 680 nm, the red one, responsible for fluorescence at around 700 nm, and the dark one, responsible for the fluorescence quenching. Our further analysis indeed confirmed this three-state model to be the minimal one describing the entirety of the experimental data [10]. We concluded that the macroscopic quenching state is related to an incoherent excitation transfer from chlorophylls (Chls) to a short-lived state of carotenoids [5]. This was in line with previous suggestions [11, 12]. On the other hand, our findings were clearly at odds with other works that suggested that the red-emitting state, which should arise from the formation of the Chl–Chl charge transfer state, is also responsible for quenching [13–16].

One key issue that might have led to different conclusions is the method of analysis applied to the experimental data. Our own analysis, presented in Ref. [5], was based on the multivariate curve resolution [17]. Most often, TRF or transient absorption data are described by means of global analysis resulting in decay-associated (difference) spectra (DA(D)S), evolution-associated (difference) spectra (EA(D)S), or species-associated (difference) spectra (SA(D)S), with the term 'difference' being applicable to differential spectroscopy, i.e. pump–probe [18]. Indeed, this type of analysis was often applied to data from LHCII trimers, LHCII aggregates, thylakoid membranes and even whole cells [12, 13, 15, 19–28]. As we have noted earlier, such analysis yields a reasonable physical interpretation only for small complexes or completely homogeneous aggregates [5, 10]. If that is not the case, the model might suggest nonexistent physical states in order to explain the experimental data. A careful analysis of the TRF of LHCII aggregates in terms of DAS/EAS is still lacking. Nonetheless, some previous works that suggested the relevance of the red-emitting state in fluorescence quenching have interpreted the global analysis of time-resolved spectroscopical data of LHCII aggregates as corresponding to the physical description [13, 15].

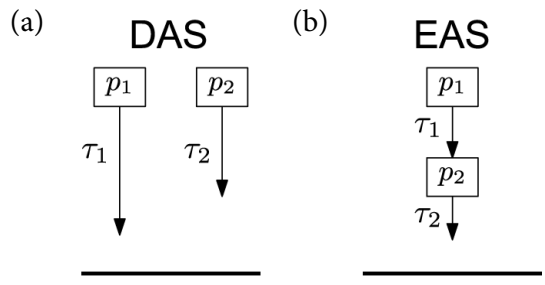

Fig. 1. Schemes depicting possible decay types of the compartmental models with two components: (a) DAS and (b) EAS.

Therefore, in this work we apply the DAS and EAS analysis to the TRF spectra of LHCII aggregates over a wide temperature range, from 273 K down to 15 K [5]. Our main goal is to investigate the information content in this type of analysis and ways for its interpretation. We find that due to the inhomogeneity of LHCII aggregates, the DAS/EAS cannot be interpreted as a physical model, but must be considered as a reduced dimensionality description of data. Nonetheless, a careful examination of this description results in the same three-state model that was presented in Ref. [5].

2. Analysis methods

Here we describe the application of DAS and EAS analysis and computational details. A more detailed discussion about these methods can be found in Ref. [18].

For both DAS and EAS, the goal is to fit the time-resolved spectroscopic data with a number of exponentially decaying components (or compartments) by finding their decay times, and then to obtain the spectra of the corresponding components. The experimentally measured fluorescence intensity function $F(\lambda, t)$ can be

expressed as a product of the spectra of the components $S_i(\lambda)$ and the time-dependent probability of their fluorescence $P_i(t)$:

$$F(\lambda,t)=\sum_{i=1}^{N}S_i(\lambda)P_i(t). \tag{1}$$

Here N is the number of components present in the system. In the matrix notation this can be written as

$$\mathbf{F}=\mathbf{S}\cdot\mathbf{P}. \tag{2}$$

Note that the time-independence of the spectral components means that the dynamic Stokes shift is not accounted for. Nonetheless, it is relevant only for early sub-ps dynamics.

In the DAS model, the system is described as a set of noninteracting compartments, each decaying with a certain decay time constant τ_i after the initial excitation (see Fig. 1(a)). For a system with N compartments we have the following equations for their populations $p_i(t)$:

$$\begin{cases}\dfrac{\mathrm{d}p_1}{\mathrm{d}t}=\dfrac{p_1}{\tau_1},\\ \dfrac{\mathrm{d}p_2}{\mathrm{d}t}=\dfrac{p_2}{\tau_2},\\ \quad\ldots\\ \dfrac{\mathrm{d}p_N}{\mathrm{d}t}=\dfrac{p_N}{\tau_N},\end{cases} \tag{3}$$

yielding N independent exponential solutions. Since the compartments surely fluoresce right after the excitation, we set the initial condition as $p_1(0)=p_2(0)=\ldots=p_N(0)=1$.

The EAS model, on the other hand, implies that only one compartment is initially excited (see Fig. 1(b)). As it decays, it sequentially excites the next compartments causing them to fluoresce. In this case the equations for $p_i(t)$ for a system with N compartments are

$$\begin{cases}\dfrac{\mathrm{d}p_1}{\mathrm{d}t}=-\dfrac{p_1}{\tau_1},\\ \dfrac{\mathrm{d}p_2}{\mathrm{d}t}=\dfrac{p_1}{\tau_1}-\dfrac{p_2}{\tau_2},\\ \quad\ldots\\ \dfrac{\mathrm{d}p_N}{\mathrm{d}t}=\dfrac{p_{N-1}}{\tau_{N-1}}-\dfrac{p_N}{\tau_N}.\end{cases} \tag{4}$$

Following the idea of the model, we require that $p_1(0)=1$ and $p_i(0)=0$, $i=2,3,\ldots,N$.

Having solved the system (3) or (4) depending on the chosen model, one has to find the τ_i constants by solving a minimization problem. Before that, however, it is necessary to take into consideration the fact that the detector used to carry out the experiment is non-ideal and cannot respond to exposure immediately. Thus, the output of the measuring device should be regarded as a convolution of the input signal and the instrument response function (IRF), which is an inherent characteristic of the detector. To account for the IRF, each of the functions p_i must be convolved with it to present a closer reproduction of the experimental data:

$$P_i(t)=\mathrm{IRF}(t)*p_i(t)=\int_0^t\mathrm{IRF}(t')p_i(t-t')\mathrm{d}t'. \tag{5}$$

In our work we used the Gaussian function as an approximation of the IRF. The full width at half maximum (FWHM) of the Gaussian was taken to be fixed, while the mean, determining the location of the maximum of the function, was used as an additional fit parameter.

The values of the functions $P_i(t)$ constitute the $N\times M$ matrix $\mathbf{P}$, where N is the number of compartments and M is the number of time points at which the fluorescence has been measured (i.e. the number of columns in the original matrix $\mathbf{F}$). The knowledge of the matrix $\mathbf{P}$ allows us to compute the spectral matrix $\mathbf{S}=\mathbf{F}\cdot\mathbf{P}^{+}$ by using the pseudo-inverse matrix $\mathbf{P}^{+}$ (see Ref. [29]). Then we reconstruct the fluorescence matrix $\mathbf{S}\cdot\mathbf{P}$ and compare it to the original data matrix $\mathbf{F}$ by finding the deviation matrix

$$\mathbf{D}=\mathbf{F}-\mathbf{S}\cdot\mathbf{P}. \tag{6}$$

Now our goal is to minimize the matrix $\mathbf{D}$ by fitting the τ_i constants to make the sum of all elements of $\mathbf{D}$ as close to 0 as possible. The explicit formula used for calculations is

$$D=\sum_{\lambda,t}\left(\mathbf{F}_{\lambda,t}-\sum_{i=1}^{N}\mathbf{S}_{\lambda,i}\mathbf{P}_{i,t}\right)^2, \tag{7}$$

where D is the parameter we seek to minimize.

To perform the minimization, we applied the Nelder–Mead downhill simplex method as a suitable solution for the cases where no *a priori*

knowledge of the function is available. Since the success of finding the global minimum using this algorithm depends greatly on the starting point, we also adopted the Genetic Algorithm which requires only an approximate possible position of the sought minimum as an input argument.

3. Results

In this section we will present the analysis of the TRF of the LHCII aggregates [5] at two temperatures, namely 50 and 150 K. These two cases represent a typical behaviour of the measured TRF spectra. The FWHM of the IRF was set to 90 ps, following Ref. [5]. Data at other temperatures was also analysed, but the results are not shown.

Figure 2(a) shows the experimental data of the TRF measurements of LHCII aggregates at 50 K temperature. The major band of interest is at about the 680 nm mark, where the LHCII trimers both absorb and fluoresce intensively [5]. As we can see, the rate of decay at the 680 nm wavelength (where the studied aggregates are known to feature a local absorption maximum) is much greater than at longer wavelengths. Meanwhile, the band at 700 nm clearly lives much longer (see Fig. 2(c) for fluorescence kinetics). The DAS and EAS models were applied to the data in order to obtain the decay constants of the components present in the system allowing us to reconstruct the fluorescence evolution and get an insight into the system. The reconstructed intensity map given by the three-component DAS model shown in Fig. 2(d) reproduces all the essential details of the original data providing a similar picture. The EAS model yielded an identical map and is therefore not shown. Since both models describe the system in a similar way in many aspects, we

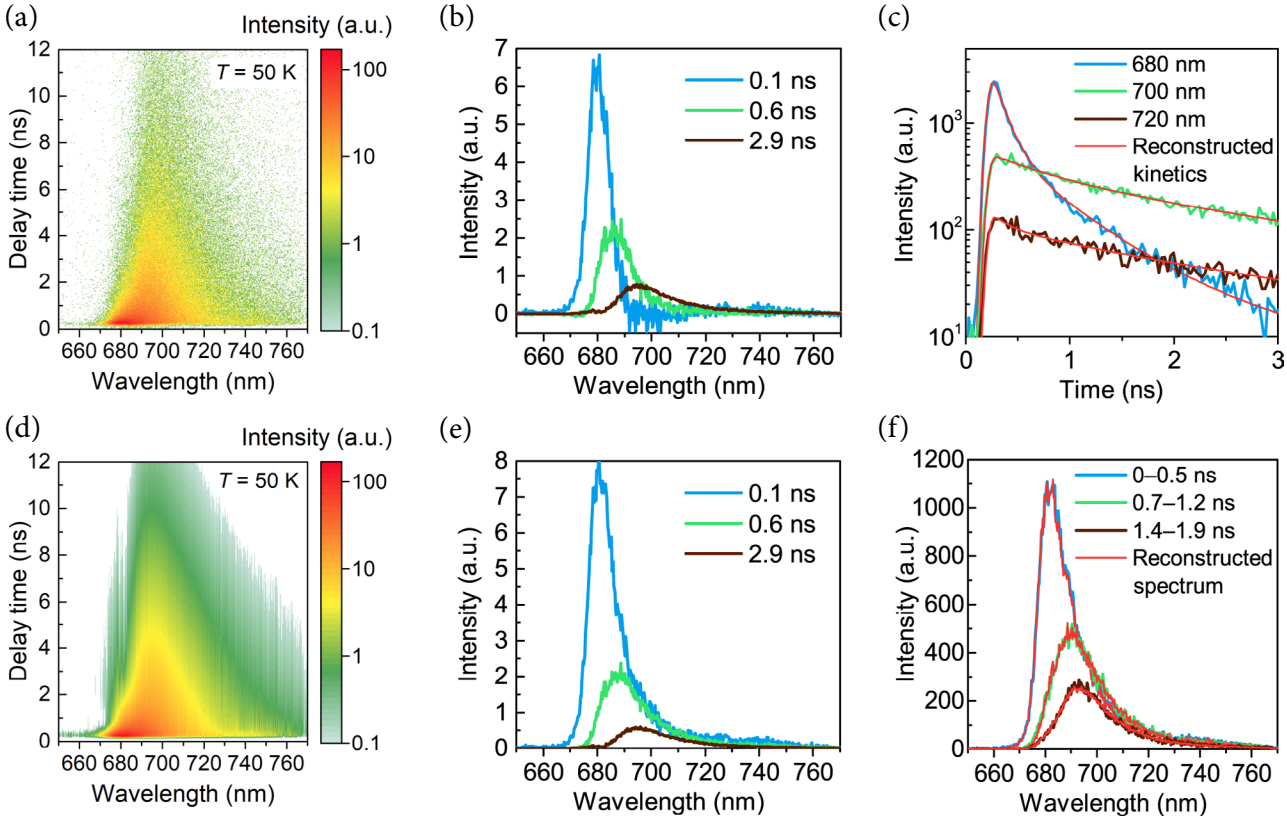

Fig. 2. Fluorescence measurement of the LHCII aggregates at 50 K temperature and its analysis. Experimental data of the fluorescence intensity measurement (a) [5]. The spectra of the components of the system obtained using the DAS model (b). Fluorescence decay kinetics integrated over a 6 nm wide region centered at the specified wavelengths as given by the measurements and the reconstructed kinetics of the DAS model. The EAS model exhibited a similar quality of the reconstructed kinetics (c). A reconstructed fluorescence intensity plot (d). The spectra of the components of the system obtained using the EAS model (e). The fluorescence spectra integrated over the specified time period as given by the measurements and the reconstructed spectra of the DAS model. The EAS model exhibited a similar quality of the reconstructed spectra (f).

present only the results given by the DAS analysis in the cases where the EAS returned the same data.

In order to evaluate the studied models we used the experimental data and the data given by the DAS/EAS to plot the decay kinetics, obtained by integrating the two-dimensional fluorescence maps $F(\lambda, t)$ over a 6 nm wide region centered at the specified wavelengths (Fig. 2(c)). The lines representing the reconstructed kinetics match the kinetics of the measured data. Analogously, Fig. 2(f) represents the spectra of the fluorescence, obtained by integrating $F(\lambda, t)$ over the specified time interval. Again, the reconstructed spectra are in a perfect agreement with the experiment.

The analysis has shown that a set of three components is sufficient to describe the behaviour of the system at 50 K. The spectra of the components of the DAS and EAS models and their decay time constants are shown in Fig. 2(b, e), respectively. One can notice that the two models gave different results here. The DAS model provided the components with slightly narrower spectra and one component featuring negative intensity values. The decay constants are the same in both cases. Another important result is that the less intensively fluorescing components with longer decay times have their maximum intensity values shifted towards the region of longer wavelengths.

The set of plots in Fig. 3 represents the data of the experiment conducted at 150 K and its analysis. The fluorescence map (Fig. 3(a)) clearly exhibits two separate peaks and shows a faster decay. Just two components were enough to reproduce the measured data (see Fig. 3(d)) and once again the DAS and EAS yielded different spectra of

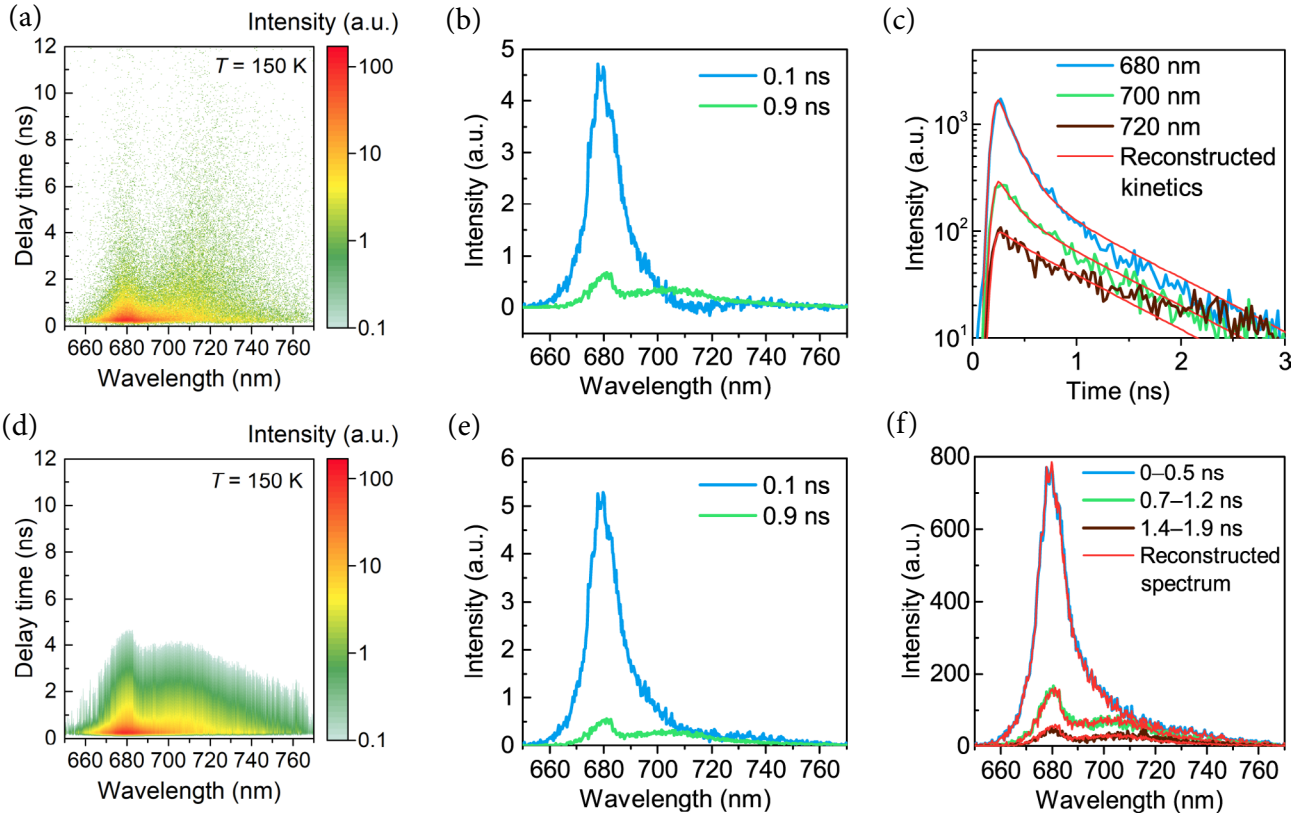

Fig. 3. Fluorescence measurement of the LHCII aggregates at 150 K temperature and its analysis. Experimental data of the fluorescence intensity measurement (a) [5]. The spectra of the components of the system obtained using the DAS model (b). Fluorescence decay kinetics integrated over a 6 nm wide region centered at the specified wavelengths as given by the measurements and the reconstructed kinetics of the DAS model. The EAS model exhibited a similar quality of the reconstructed kinetics (c). A reconstructed fluorescence intensity plot (d). The spectra of the components of the system obtained using the EAS model (e). The fluorescence spectra integrated over the specified time period as given by the measurements and the reconstructed spectra of the DAS model. The EAS model exhibited a similar quality of the reconstructed spectra (f).

the components, shown in Fig. 3(b, e), respectively. The decay constants of the components are similar to those obtained from the 50 K temperature experiment analysis, but this time both components have their intensity maxima at approximately the same 680 nm mark. The reconstructed kinetics in Fig. 3(c) are accurate up to 2 ns. The divergence between the fitting curve and the experimental data at later times comes as a result of the compartments decaying almost completely in the first 2 ns. At times up to 2 ns the integrated spectra (see Fig. 3(f)) repeat the original data accurately.

By looking at the spectra of the components computed from the 50 K experiment data (Fig. 2(b, e)) we can notice that each component has only one clearly distinguishable intensity maximum. The most intensively fluorescing component with a maximum at approximately 680 nm is responsible for the initial burst of intense fluorescence around the 680 nm mark that can be easily seen in the measured fluorescence plot (Fig. 2(a)). The same plot also shows a rapid decay at the mentioned wavelength, which justifies the smallest decay time constant (0.1 ns) of the first component. Similarly, the slow decay seen in the fluorescence evolution plot around the 700 nm region explains the longest decay time constant (2.9 ns) of the component with a maximum at the same wavelength.

The spectra of the components obtained from the 150 K data (see Fig. 3(b, e)) differ from those discussed above. The slower of the two components features two fluorescnce bands: one around the 680 nm region and another, less intense but significantly wider, at approximately 710 nm. The latter is explained by the fluorescence measurements plot (Fig. 3(a)), in which we can see the prolonged decay of a moderately intense fluorescence around the 710 nm mark. Also, contrary to the case of 50 K experiment, here the system did not decay too quickly in the 680 nm region (where the fastest component has a maximum). The reason for this is evident from the spectra: the component with a longer decay time constant (0.9 ns) also has a maximum at the same wavelength and its slower decay causes the extended fluorescence.

The TRF measurements within the 15–273 K temperature range allowed us to trace some general tendencies in the fluorescence of LHCII aggregates and their modelling. At higher temperatures, the intensity of the fluorescence is notably lower than at temperatures closer to 15 K, and the system decays at a greater rate. Thus, at lower temperatures the components of the system feature longer decay times (compared to the results given by the DAS/EAS models with the same amount of compartments). At temperatures lower than 130 K the system is described more accurately when a three-compartment model is applied, which gives an additional component with a lifetime significantly longer than those of the two other components. A two-compartment model is suitable for the systems at temperatures above 130 K.

4. Discussion

4.1. Interpretation of DAS/EAS

Here we have demonstrated that both DAS and EAS analysis can be successfully applied for the TRF datasets of LHCII aggregates with reconstructed kinetics and spectra well matching the experimental data. Having previously expressed criticism for the application of DAS/EAS for this system [5, 10], let us now discuss the main issues that might arise when interpreting the obtained results.

The first point we would like to raise is that DAS/EAS can be understood in two ways. On the one hand, it is just a data dimensionality reduction technique. Indeed, one of the main goals of dataset dimensionality reduction is to find new variables, which can be used to express the same data more succinctly [30]. In the case of DAS/EAS this is achieved by obtaining N one-dimensional spectra with their corresponding timescales instead of a full two-dimensional time- and wavelength-resolved data matrix. Clearly, this type of decomposition can be readily achieved for most of the spectroscopically studied systems. Our results from Figs. 2 and 3 show that this is indeed the case for the LHCII aggregates. Viewing DAS/EAS in this light the results will never be 'wrong', but care must be taken with their interpretation.

The situation is somewhat different if DAS/EAS are understood as representing a physical kinetic model. For this the data must satisfy several assumptions [18], that, unfortunately, are sometimes forgotten. The first assumption is that

the time and wavelength properties of the system can be separated. In other words, this means that the spectra of each species present in the sample are constant in time. Physically, this means ignoring effects like dynamic Stokes shift, which, however, is usually not a problem since it happens extremely fast (tens to hundreds of femtoseconds) if compared to timescales of a typical TRF experiment (tens to hundreds of picoseconds or even nanoseconds). The second, and sometimes overlooked, assumption is the homogeneity of the system under consideration. In other words, each member from the measured ensemble – like a distinct molecule or a densely packed molecular aggregate (pigment–protein light-harvesting complex in our case) – must have very closely matching dynamical and spectral properties.

If we wish to interpret the DAS/EAS of the TRF of LHCII aggregates in terms of a physical model, we must make sure that both of the aforementioned assumptions are satisfied. We can with relative confidence assume that the spectra of any components in LHCII aggregates should be stationary in time, as no noticeable shifts can be seen in the TRF measurements of separate LHCII trimers [5].

The situation is completely different regarding the homogeneity of the aggregates. This property is actually assumed in the so-called homogeneous oligomer model by the Holzwarth group [13–15]. They proposed that all the monomers in LHCII aggregates are roughly the same, each of them possessing an intrinsic microscopic red-emitting state that is responsible for the fluorescence at ~700 nm. That state was also related to the fluorescence quenching [13, 15]. This type of model, however, is immediately at odds with simple absorption measurements of LHCII aggregates, which show no significant increase in absorption in the spectral region corresponding to the red state [5]. We have recently analysed the homogeneous oligomer model in detail and showed that it fails to correctly describe even the TRF experiments, especially for longer times [10].

On the other hand, the inhomogeneity of LHCII aggregates can be assumed for physical reasons. First, as mentioned above, the relative concentration of the red-emitting species in the aggregate must be limited. Therefore, from statistical grounds it follows that the exact number or red-emitting complexes in each particular aggregate in the ensemble is a random number, which naturally results in some level of static inhomogeneity. Furthermore, the exact sizes of the aggregates and the positions of the red-emitting complexes therein are also likely to have some distributions. Note that single-molecule spectroscopy experiments have demonstrated that due to conformational dynamics of the protein scaffold even separated LHCII trimers can switch reversibly between different emitting and/or quenching states on the timescale of milliseconds [9, 31]. The streak camera measurements themselves typically require up to several tens of minutes to be performed in order to maintain a reasonable signal-to-noise ratio in the gathered TRF spectra. As a result, during the measurement time the number of LHCII complexes being in different conformational states naturally fluctuates even within the same aggregate, thus being the source of dynamic inhomogeneity.

The degree of inhomogeneity in LHCII aggregates must be assumed to be even higher once we take into account that there exists separate non-emitting conformational states responsible for excitation quenching, as demonstrated in [5] and confirmed in [10]. Then all the aforementioned considerations for the red-emitting states would apply for the quenching states as well. Moreover, co-existance of several independent quenching mechanisms has been reported recently [32], which might be important while studying *in vivo* light-harvesting systems.

We must therefore conclude that inhomogeneity of LHCII aggregates can be readily assumed. Thus, the DAS/EAS of their TRF spectra cannot be taken to be related to a physical model, but must instead be understood as a purely mathematical technique allowing one to describe the whole dataset with just several simple quantities – several spectral components together with their mean lifetimes.

4.2. Information content of DAS/EAS of TRF of LHCII aggregates

Having argued that the DAS/EAS of the TRF of LHCII aggregates must be taken solely as a reduced data description, we can nonetheless analyse what this description can tell us. Indeed, it is easier to

analyse a set of one-dimensional spectra and their lifetimes (Figs. 2(b, e) and 3(b, e)) than a full two-dimensional map of data (Figs. 2(a) and 3 (a)). Then our goal is to suggest the simplest possible model of the LHCII aggregate that is consistent with DAS/EAS. In this consideration we must always have in mind the LHCII aggregate absorption data and the TRF data from LHCII trimers [5].

Let us begin by analysing the 50 K data, shown in Fig. 2. First of all, both DAS and EAS show that the dominant fluorescent peak at ~680 nm decays very rapidly, with a timescale of 100 ps. Physically, the decay can be due to either relaxation from the fluorescent state to the ground state or due to energy transfer to species that fluoresce at other wavelengths or do not fluoresce at all.

We must note, however, that the word 'state' can be somewhat ambiguous. It can mean either a microscopic state within an LHCII monomer binding 14 chlorophyll molecules or a macroscopic (conformational) state of the whole complex. The simplest coarse-grained description corresponds to an assumption that every complex can be described by a single state. Since the intra-complex excitation equilibration is expected to be very fast, on the order of several picoseconds [33, 34], this assumption is justified when we are dealing with TRF experiments and the timescales of hundreds of picoseconds. Therefore, hereafter the word 'state' will correspond to a macroscopic state of a single LHCII complex in the aggregate, and energy transfer will be considered among different neighbouring complexes.

Coming back to the analysis of DAS/EAS, the origin of the fluorescent state in the LHCII aggregates should be the same as in the LHCII trimers. Since the TRF of the latter decays with a lifetime of 4–5 ns [5], we can relatively safely assume that the non-radiative decay rate of the fluorescent state could not increase so much due to the aggregation process. Therefore, the decay of the dominating 680 nm peak must be related to the energy transfer in the aggregate.

We must take into account that the amplitude of the 690 nm peak from the second DAS/EAS component is considerably smaller than that of the 680 nm peak (compare 0.1 and 0.6 ns EAS components in Fig. 2(e)), and the amplitude of the 700 nm peak from the third DAS/EAS is smaller still. The simplest explanation is that the effective transition dipole moment of the red-emitting state(s) could be much smaller than that of the 680 nm state. A question now arises whether there exists an intermediate state fluorescing at ~690 nm. Looking over both DAS and EAS in Fig. 2(b, e), we see a steady redshift in the maximum of the fluorescence. This could be interpreted as there being an intermediate state between 680 and 700 nm. A simpler explanation, however, is that the appearance of the intermediate state is just an artefact of non-exponential kinetics and merely represents times when the amplitudes of 680 and 700 nm peaks are comparable. Having in mind that the system under consideration should be inhomogeneous, the latter explanation is more likely.

The above consideration leads to a model of the aggregate with two states: the first one fluoresces at 680 nm and has non-radiative decay similar to that of LHCII trimers, while the second fluoresces at 700 nm, has a smaller effective transition dipole moment and exhibits a much shorter lifetime to account for the overall faster decay of fluorescence in aggregates versus trimers. This seems the simplest model that can be constructed from the analysis of DAS/EAS that is consistent with the experimental data. Indeed, this model was analysed in detail in Ref. [10], and it was shown that after accounting for the inhomogeneity of the aggregate this model could in principle explain the TRF of LHCII aggregates.

Nevertheless, as mentioned above, we must ask whether this model can also explain the absorption spectra of the aggregates and the TRF of LHCII trimers. Since the decay of the population of the state fluorescing at 680 nm is quite rapid, this means that the relative concentration of the quenching complexes in the aggregate cannot be negligible. If these quenching complexes were to fluoresce, as is assumed in the simplest model described above, the TRF of the trimers would also show non-exponential kinetics, which is not the case [5]. Also, we must remember that the absorption of LHCII aggregates has no increase in amplitude at ~700 nm [5], implicating that either the relative concentration of the red-emitting complexes is negligible or that their effective transition dipole moment is negligible. Yet from the TRF data we see that the number of quenching complexes is clearly distinguishable

and that the effective transition dipole moment of the red-emitting complexes cannot be neglected. These considerations lend an additional weight to the argument that the two-state model does not account for the totality of the experimental data.

A slightly more complicated model that is consistent with the above considerations would include an additional dark or quenching state. Thus, some complexes in the aggregate would fluoresce at 680 nm, some at 700 nm and some would be dark and not fluoresce at all. Both emitting states could have the same non-radiative lifetime. In this way the TRF of LHCII trimers would show only exponential kinetics, while the lack of a red shoulder in the aggregate absorption spectra can be explained by a relatively low concentration of complexes in the red-emitting state.

Let us now turn to the 150 K data, given in Fig. 3. The situation in this case is different, because only two components were enough to describe the TRF data. The first DAS/EAS (Fig. 3(b, e)), however, is relatively similar to the 50 K case, demonstrating a strong fluorescence at ~680 nm and having a similar fast timescale. The second component has features at both 680 and 700–720 nm. These features are consistent with the three-state model described above. The inmogeneity of the aggregate is then responsible for the non-exponential character of the 680 nm peak kinetics, while fluorescence from 700–720 nm comes from the complexes in the red-emitting state.

We therefore find that a careful consideration of DAS/EAS of the TRF of LHCII aggregates taken together with the absorption data as well as the results from LHCII trimers leads to the same three-state model that we proposed in Ref. [5]. In that work we used the multivariate curve resolution [17] for data analysis. This method has an advantage over the DAS/EAS analysis that the homogeneity of the investigated system is not required, thus the obtained kinetics and spectra could be attributed to physical states in the LHCII aggregate. Nonetheless, as we demonstrate here, when the DAS/EAS analysis is performed carefully, the same conclusions can be reached.

5. Conclusions

In this work we investigated the TRF of LHCII aggregates in terms of the DAS/EAS. Even though the LHCII aggregates are obviously not homogeneous (thus one of the requirements for DAS/EAS to correspond to a physical model is not fulfilled), these analysis methods still represent a valid reduced dimensionality data description. To reveal the physical picture beyond the TRF dataset, however, solely performing this kind of analysis is not sufficient, and supplementary knowledge about the considered system becomes necessary. Indeed, interpreting the DAS/EAS in such light and having in mind other spectroscopic data, we come to the conclusion that a three-state model of the LHCII aggregate is the simplest one that can explain the totality of the data. This agrees with our previous works.

Naturally, misinterpretation of DAS/EAS might lead to erroneous conclusions, which occur when the necessary requirements for DAS/EAS to correspond to a physical model are neglected. On the other hand, even in those circumstances DAS/EAS can be viewed just as a reduced description of the spectroscopic data, which can then be a suitable starting point for further analysis.

Acknowledgements

The authors acknowledge the Lithuanian-Ukrainian grant S-LU-18-7 for the financial support and thank Egidijus Songaila and Ramūnas Augulis for the experimental measurements. Y. B. acknowledges funding by the European Social Fund under Measure No. 09.3.3- LMT-K-712 'Development of Competences of Scientists, other Researchers and Students through Practical Research Activities'.

References

[1] R.E. Blankenship, *Molecular Mechanisms of Photosynthesis*, 2nd ed. (Wiley Blackwell, Chichester, 2014).

[2] A.V. Ruban, M.P. Johnson, and Ch.D.P. Duffy, The photoprotective molecular switch in the photosystem II antenna, Biochim. Biophys. Acta **1817**, 167–181 (2012).

[3] Ch.D.P. Duffy and A.V. Ruban, Dissipative pathways in the photosystem-II antenna in plants, J. Photochem. Photobiol. B **152**, 215–226 (2015).

[4] T.K. Ahn, T.J. Avenson, M. Ballottari, Y.C. Cheng, K.K. Niyogi, R. Bassi, and G.R. Fleming, Architecture of a charge-transfer state regulating

light harvesting in a plant antenna protein, Science **320**, 794–797 (2008).

[5] J. Chmeliov, A. Gelzinis, E. Songaila, R. Augulis, Ch.D.P. Duffy, A.V. Ruban, and L. Valkunas, The nature of self-regulation in photosynthetic light-harvesting antenna, Nat. Plants **2**, 16045 (2016).

[6] P. Horton, A.V. Ruban, D. Rees, A.A. Pascal, G. Noctor, and A.J. Young, Control of the light-harvesting function of chloroplast membranes by aggregation of the LHCII chlorophyll–protein complex, FEBS Lett. **292**, 1–4 (1991).

[7] A.V. Ruban, A. Young, and P. Horton, Modulation of chlorophyll fluorescence quenching in isolated light harvesting complex of Photosystem II, Biochim. Biophys. Acta **1186**, 123–127 (1994).

[8] T.P.J. Krüger, C. Ilioaia, M.P. Johnson, A.V. Ruban, E. Papagiannakis, P. Horton, and R. van Grondelle, Controlled disorder in plant light-harvesting complex II explains its photoprotective role, Biophys. J. **102**, 2669–2676 (2012).

[9] T.P.J. Krüger, C. Ilioaia, M.P. Johnson, A.V. Ruban, and R. van Grondelle, Disentangling the low-energy states of the major light-harvesting complex of plants and their role in photoprotection, Biochim. Biophys. Acta **1837**, 1027–1038 (2014).

[10] A. Gelzinis, J. Chmeliov, A.V. Ruban, and L. Valkunas, Can red-emitting state be responsible for fluorescence quenching in LHCII aggregates? Photosynth. Res. **135**, 275–284 (2018).

[11] A.A. Pascal, Z.F. Liu, K. Broess, B. van Oort, H. van Amerongen, C. Wang, P. Horton, B. Robert, W.R. Chang, and A. Ruban, Molecular basis of photoprotection and control of photosynthetic light-harvesting, Nature **436**, 134–137 (2005).

[12] A.V. Ruban, R. Berera, C. Ilioaia, I.H.M. van Stokkum, J.T.M. Kennis, A.A. Pascal, H. van Amerongen, B. Robert, P. Horton, and R. van Grondelle, Identification of a mechanism of photoprotective energy dissipation in higher plants, Nature **450**, 575–578 (2007).

[13] Y. Miloslavina, A. Wehner, P.H. Lambrev, E. Wientjes, M. Reus, G. Garab, R. Croce, and A.R. Holzwarth, Far-red fluorescence: A direct spectroscopic marker for LHCII oligomer formation in non-photochemical quenching, FEBS Lett. **582**, 3625–3631 (2008).

[14] A.R. Holzwarth, Y. Miloslavina, M. Nilkens, and P. Jahns, Identification of two quenching sites active in the regulation of photosynthetic light-harvesting studied by time-resolved fluorescence, Chem. Phys. Lett. **483**, 262–267 (2009).

[15] M.G. Müller, P. Lambrev, M. Reus, E. Wientjes, R. Croce, and A.R. Holzwarth, Singlet energy dissipation in the photosystem II light-harvesting complex does not involve energy transfer to carotenoids, Chem. Phys. Chem. **11**, 1289–1296 (2010).

[16] A. Kell, X. Feng, C. Lin, Y. Yang, J. Li, M. Reus, A.R. Holzwarth, and R. Jankowiak, Charge-transfer character of the low-energy Chl *a* Q_y absorption band in aggregated light harvesting complexes II, J. Phys. Chem. B **118**, 6086–6091 (2014).

[17] W.H. Lawton and E.A. Sylvestre, Self modeling curve resolution, Technometrics **13**, 617–633 (1971).

[18] I.H.M. van Stokkum, D.S. Larsen, and R. van Grondelle, Global and target analysis of time-resolved spectra, Biochim. Biophys. Acta **1657**, 82–104 (2004).

[19] C.W. Mullineaux, A.A. Pascal, P. Horton, and A.R. Holzwarth, Excitation-energy quenching in aggregates of the LHC II chlorophyll-protein complex: a time-resolved fluorescence study, Biochim. Biophys. Acta **1141**, 23–28 (1993).

[20] J.P. Connelly, M.G. Müller, M. Hucke, G. Gatzen, C.W. Mullineaux, A.V. Ruban, P. Horton, and A.R. Holzwarth, Ultrafast spectroscopy of trimeric light-harvesting complex II from higher plants, J. Phys. Chem. B **101**, 1902–1909 (1997).

[21] S. Vasil'ev, K.-D. Irrgang, T. Schrötter, A. Bergmann, H.-J. Eichler, and G. Renger, Quenching of chlorophyll *a* fluorescence in the aggregates of LHCII: Steady state fluorescence and picosecond relaxation kinetics, Biochemistry **36**, 7503–7512 (1997).

[22] I. Moya, M. Silvestri, O. Vallon, G. Cinque, and R. Bassi, Time-resolved fluorescence analysis of the photosystem II antenna proteins in detergent

micelles and liposomes, Biochemistry **40**, 12552–12561 (2001).

[23] M.A. Palacios, J. Standfuss, M. Vengris, B.F. van Oort, I.H.M. van Stokkum, W. Kühlbrandt, H. van Amerongen, and R. van Grondelle, A comparison of the three isoforms of the light-harvesting complex II using transient absorption and time-resolved fluorescence measurements, Photosynth. Res. **88**, 269–285 (2006).

[24] C.D. van der Weij-de Wit, J.A. Ihalainen, R. van Grondelle, and J.P. Dekker, Excitation energy transfer in native and unstacked thylakoid membranes studied by low temperature and ultrafast fluorescence spectroscopy, Photosynth. Res. **93**, 173–182 (2007).

[25] M. Fuciman, M.M. Enriquez, T. Polívka, L. Dall'Osto, R. Bassi, and H.A. Frank, Role of xanthophylls in light harvesting in green plants: A spectroscopic investigation of mutant LHCII and Lhcb pigment–protein complexes, J. Phys. Chem. B **116**, 3834–3849 (2012).

[26] N.M. Magdaong, M.M. Enriquez, A.M. LaFountain, L. Rafka, and H.A. Frank, Effect of protein aggregation on the spectroscopic properties and excited state kinetics of the LHCII pigment–protein complex from green plants, Photosynth. Res. **118**, 259–276 (2013).

[27] L. Tian, E. Dinc, and R. Croce, LHCII populations in different quenching states are present in the thylakoid membranes in a ratio that depends on the light conditions, J. Phys. Chem. Lett. **6**, 2339–2344 (2015).

[28] B. van Oort, R. van Grondelle, and I.H.M. van Stokkum, A hidden state in light-harvesting complex II revealed by multipulse spectroscopy, J. Phys. Chem. B **119**, 5184–5193 (2015).

[29] V.I. Prokhorenko, in: *EPA (European Photochemistry Association) Newsletter* (Media Services, UK, June 2012) pp. 21–23.

[30] Ch. Chatfield and A.J. Collins, *Introduction to Multivariate Analysis* (Chapman & Hall/CRC, London, 1980).

[31] T.P.J. Krüger, V.I. Novoderezkhin, C. Ilioaia, and R. van Grondelle, Fluorescence spectral dynamics of single LHCII trimers, Biophys. J. **98**, 3093–3101 (2010).

[32] L. Dall'Osto, S. Cazzaniga, M. Bressan, D. Paleček, K. Židek, K.K. Niyogi, G.R. Fleming, D. Zigmantas, and R. Bassi, Two mechanisms for dissipation of excess light in monomeric and trimeric light-harvesting complexes, Nat. Plants **3**, 17033 (2017).

[33] V.I. Novoderezhkin, M.A. Palacios, H. van Amerongen, and R. van Grondelle, Excitation dynamics in the LHCII complex of higher plants: Modeling based on the 2.72 Å crystal structure, J. Phys. Chem. B **109**, 10493–10504 (2005).

[34] F. Müh, M. El-Amine Madjet, and Th. Renger, Structure-based identification of energy sinks in plant light-harvesting complex II, J. Phys. Chem. B **114**, 13517–13535 (2010).

LHCII AGREGATŲ LAIKINĖS SKYROS FLUORESCENCIJOS GESIMO IR EVOLIUCIJOS SPEKTRAI

A. Gelzinis [a, b], J. Braver [a, b], J. Chmeliov [a, b], L. Valkunas [a, b]

[a] *Vilniaus universiteto Fizikos fakulteto Cheminės fizikos institutas, Vilnius, Lietuva*

[b] *Fizinių ir technologijos mokslų centro Molekulinių darinių fizikos skyrius, Vilnius, Lietuva*

Santrauka

Laikinės skyros fluorescencijos spektrų matavimas yra vienas iš populiariausių eksperimentinių metodų, taikomų siekiant išsiaiškinti įvairiose molekulinėse sistemose vykstančių fotoindukuotų vyksmų dinamiką ir ją nulemiančius fizikinius mechanizmus. Neseniai publikuotame darbe [Chmeliov et al., Nat. Plants **2**, 16045 (2016)] buvo pristatyti augalų fotosintetinių pigmentų ir baltymų anteninių kompleksų (LHCII) agregatų laikinės skyros fluorescencijos spektrai, išmatuoti esant plačiam temperatūriniam intervalui, o šių duomenų išsami analizė leido atskleisti už nefotocheminį gesinimą atsakingo augalų fotoapsaugos mechanizmo molekulinę prigimtį. Laikinės skyros spektrams interpretuoti plačiai taikomi globaliosios analizės metodai (tokie kaip gesimo ar evoliucijos spektrų skaičiavimas), tačiau priklausomai nuo tiriamos sistemos sudėtingumo jie ne visada sukuria teisingą toje sistemoje vykstančių reiškinių fizikinį vaizdinį. Darbe šie metodai pritaikomi minėtiems LHCII agregatų laikinės skyros fluorescencijos spektrams aprašyti. Parodoma, kad nors pateikiami matematiškai teisingi eksperimentinių duomenų aprašymai, dėl sistemos nehomogeniškumo tinkamai interpretuoti galima tik atsižvelgiant į papildomus spektroskopinius duomenis.